Targeting CXCR7/ACKR3 as a therapeutic strategy to promote remyelination in the adult central nervous system

Jessica L. Williams,[1] Jigisha R. Patel,[1] Brian P. Daniels,[3] and Robyn S. Klein[1,2,3]

[1]Department of Internal Medicine, [2]Department of Pathology and Immunology, and [3]Department of Anatomy and Neurobiology, Washington University School of Medicine, St. Louis, MO 63110

Current treatment modalities for the neurodegenerative disease multiple sclerosis (MS) use disease-modifying immunosuppressive compounds but do not promote repair. Although several potential targets that may induce myelin production have been identified, there has yet to be an approved therapy that promotes remyelination in the damaged central nervous system (CNS). Remyelination of damaged axons requires the generation of new oligodendrocytes from oligodendrocyte progenitor cells (OPCs). Although OPCs are detected in MS lesions, repair of myelin is limited, contributing to progressive clinical deterioration. In the CNS, the chemokine CXCL12 promotes remyelination via CXCR4 activation on OPCs, resulting in their differentiation into myelinating oligodendrocytes. Although the CXCL12 scavenging receptor CXCR7/ACKR3 (CXCR7) is also expressed by OPCs, its role in myelin repair in the adult CNS is unknown. We show that during cuprizone-induced demyelination, in vivo CXCR7 antagonism augmented OPC proliferation, leading to increased numbers of mature oligodendrocytes within demyelinated lesions. CXCR7-mediated effects on remyelination required CXCR4 activation, as assessed via both phospho-S339-CXCR4–specific antibodies and administration of CXCR4 antagonists. These findings identify a role for CXCR7 in OPC maturation during remyelination and are the first to use a small molecule to therapeutically enhance myelin repair in the demyelinated adult CNS.

CORRESPONDENCE
Robyn S. Klein:
rklein@dom.wustl.edu

Abbreviations used: CC, corpus callosum; CNS, central nervous system; CPZ, cuprizone; CXCR7, CXCR7/ACKR3; MBP, myelin basic protein; MOG, myelin oligodendrocyte glycoprotein; MS, multiple sclerosis; OPC, oligodendrocyte progenitor cell.

Multiple sclerosis (MS) is a progressive, neurodegenerative disease of the central nervous system (CNS) in which myelin destruction leads to motor and sensory function loss. A majority of MS patients present with remitting-relapsing disease, characterized by periods of demyelination followed by partial recovery (Steinman, 2009). Despite the presence of oligodendrocyte progenitor cells (OPCs) in MS lesions (Chang et al., 2000, 2002), remyelination gradually fails while demyelination continues, contributing to progressive clinical deterioration (Compston and Coles, 2002). The mechanisms underlying CNS repair are poorly understood; thus, there are currently no therapies to augment remyelination (Franklin and Ffrench-Constant, 2008).

Recent data indicate that the chemokine CXCL12 regulates OPC-mediated remyelination (Carbajal et al., 2010; Patel et al., 2010, 2012). CXCL12 and its receptor, CXCR4, are indispensable for the plasticity of the CNS (Zou et al., 1998; Zhu et al., 2009) as they are necessary for proper migration and survival of OPCs (Dziembowska et al., 2005). Blockade of CXCR4-CXCL12 signaling limits OPC maturation during remyelination (Carbajal et al., 2010; Patel et al., 2010). An alternative CXCL12 scavenger receptor, CXCR7/ACKR3 (CXCR7), sequesters ligand for degradation, regulating CXCL12-mediated activation of CXCR4 (Boldajipour et al., 2008; Naumann et al., 2010; Cruz-Orengo et al., 2011b). In vitro studies of OPCs reveal functional expression of CXCR7 (Göttle et al., 2010), suggesting that it may regulate CXCR4 activation during differentiation, as is observed for other neural progenitors (Boldajipour et al., 2008). The in vivo role of CXCR7 within the demyelinated CNS remains largely unexamined.

The Rockefeller University Press $30.00
J. Exp. Med. 2014 Vol. 211 No. 5 791-799
www.jem.org/cgi/doi/10.1084/jem.20131224

The Journal of Experimental Medicine

Our previous studies demonstrate that CXCR7 targeting during experimental autoimmune encephalomyelitis (EAE) decreases disease severity as a result of altered T cell localization in the perivascular space, restricting autoreactive leukocyte trafficking into the CNS parenchyma (Cruz-Orengo et al., 2011b). In vivo analysis revealed that CXCR7 antagonism during EAE also preserves axonal integrity (Cruz-Orengo et al., 2011a). In the current study, we investigated the role of CXCR7 during demyelination and remyelination in the context of cuprizone (CPZ) exposure. During CPZ-mediated myelin injury, OPCs migrate to and proliferate within the caudal corpus callosum (CC) to initiate repair (Patel et al., 2010). After cessation of CPZ, OPCs differentiate into mature oligodendrocytes and remyelination is achieved within weeks (Lindner et al., 2008). We report that during demyelination, CXCR7 expression is significantly up-regulated, returning to baseline during remyelination. Treatment with CCX771, a specific CXCR7 antagonist (Cruz-Orengo et al., 2011b), during demyelination and peak CXCR7 expression led to increased levels of CXCL12, enhanced CXCR4 activation and augmented differentiation of OPCs, resulting in increased numbers of mature oligodendrocytes within the demyelinated CC. The enhanced remyelination observed in CCX771-treated animals was abrogated by treatment with the specific CXCR4 antagonist AMD3100 (Hatse et al., 2002). These data indicate that CXCR7 regulates CXCL12-CXCR4–mediated CNS myelin repair and may therefore serve as a valuable therapeutic target to promote remyelination in the demyelinated adult CNS.

RESULTS AND DISCUSSION

Expression of CXCL12 and its receptors, CXCR4 and CXCR7, is increased during repair of myelin within the adult CNS

To evaluate the effects of demyelination on CXCR7 expression, we evaluated the corpus callosum of CPZ-exposed mice in which one copy of the CXCR7 gene was replaced with cDNA encoding enhanced GFP ($CXCR7^{GFP/+}$; Cruz-Orengo et al., 2011b) at 0, 3, and 6 wk after CPZ exposure and at 10 d after CPZ cessation. During demyelination, as myelin basic protein (MBP) levels decrease over time (Fig. 1 A), CXCR4, CXCR7, and CXCL12 levels were significantly increased within the CC (Fig. 1, B–D), peaking before remyelination. Importantly, during remyelination, CXCR7 levels return to those observed in naive animals (Fig. 1 B), while CXCR4 and CXCL12 levels remain elevated (Fig. 1, C and D). As previously observed, OPC numbers dramatically increase within the demyelinated CC after 3–6 wk of CPZ intoxication (Patel et al., 2010; Fig. 1 E) and diminish, as expected, during remyelination (Fig. 1 E). In accordance with prior studies, the up-regulation of CXCR7 exclusively during demyelination is consistent with its role in tightly regulating CXCR4 activity in response to extracellular CXCL12 during CNS insult (Schönemeier et al., 2008).

Several CNS cell types are known to express CXCL12 during injury and mediate pluripotent effects (Bajetto et al., 1999; Banisadr et al., 2003; Calderon et al., 2006; McCandless et al., 2008; Schönemeier et al., 2008). Given that spatiotemporal expression of CXCL12 is critical to its function during CNS injury and its levels are regulated by CXCR7, we sought to identify cellular sources of CXCR7 during demyelination. After 3 wk of CPZ intoxication, CXCR7 was expressed by OPCs (45.9 ± 8.0%) and activated astrocytes (43.1 ± 10.5%; Fig. 1 F). However, after 6 wk of CPZ, CXCR7 was expressed by multiple cell types including OPCs (28.2 ± 3.1%), activated astrocytes (30.4 ± 1.9%), endothelial cells (15.8 ± 4.2%), and axons (22.2 ± 5.7%). CXCR7 expression was minimally detected within activated microglia (1.3 ± 0.4%; Fig. 1 G). Of note, 6.2 ± 1.8% and 4.3 ± 0.7% of OPCs expressed CXCR7 after 3 and 6 wk of CPZ treatment, respectively.

CXCR7 regulates levels of CXCL12 protein and CXCR4 signaling in OPCs

The high levels of expression of CXCR7 during demyelination suggested it might serve to regulate extracellular levels of CXCL12. To test this, we administered a CXCR7 antagonist, CCX771 (Cruz-Orengo et al., 2011b), versus a vehicle control (10% captisol) to mice during the first or final 3 wk of CPZ-mediated demyelination occurring over a 6-wk period (Fig. 2, A and C). Although CXCL12 protein levels did not differ in vehicle versus CCX771-treated mice after the first 3 wk of treatment (Fig. 2 B), CXCR7 antagonism during the latter 3 wk of CPZ resulted in increased levels of CXCL12 (Fig. 2, D and F). Levels of ligand-activated CXCR4 (phospho-S339-(p)CXCR4) in OPCs were also increased in the CCX771-treated CC compared with vehicle-treated controls during demyelination (Fig. 2 E). These data suggest that the CCX771-mediated increase in CXCL12 promotes CXCR4 activation within OPCs. Because an increase in CXCL12 mRNA expression was not observed in the presence of CCX771 (Fig. 2 G) but, rather, a decrease in CXCL12-mCherry internalization in astrocytes was seen in the presence of CCX771 (Fig. 2 H), the mechanism of CCX771-mediated CXCL12 regulation is likely dependent on decreased degradation of available CXCL12 protein. The lack of effect of CCX771 on levels of CXCL12 at the 3-wk time point is likely due to the low levels of CXCR7 observed during the first 3 wk of CPZ exposure (Fig. 1 B). These findings during CNS injury are reminiscent of molecular events that occur during development wherein CXCL12 provides localization cues to neural progenitors, regulating CXCR4 signaling in precursor cells in proliferative zones within the brain (Klein and Rubin, 2004).

CXCR7 regulates the proliferation and maturation of OPCs during demyelination

Because proliferation of OPCs peaks between 3 and 4 wk of CPZ exposure (Arnett et al., 2001), we determined whether CXCR7 inactivation impacted OPC proliferation during demyelination. To evaluate the influence of CXCR7 on OPC proliferation, mice were fed CPZ-infused feed and treated with CCX771, followed by BrdU injections every 8 h for 4 d

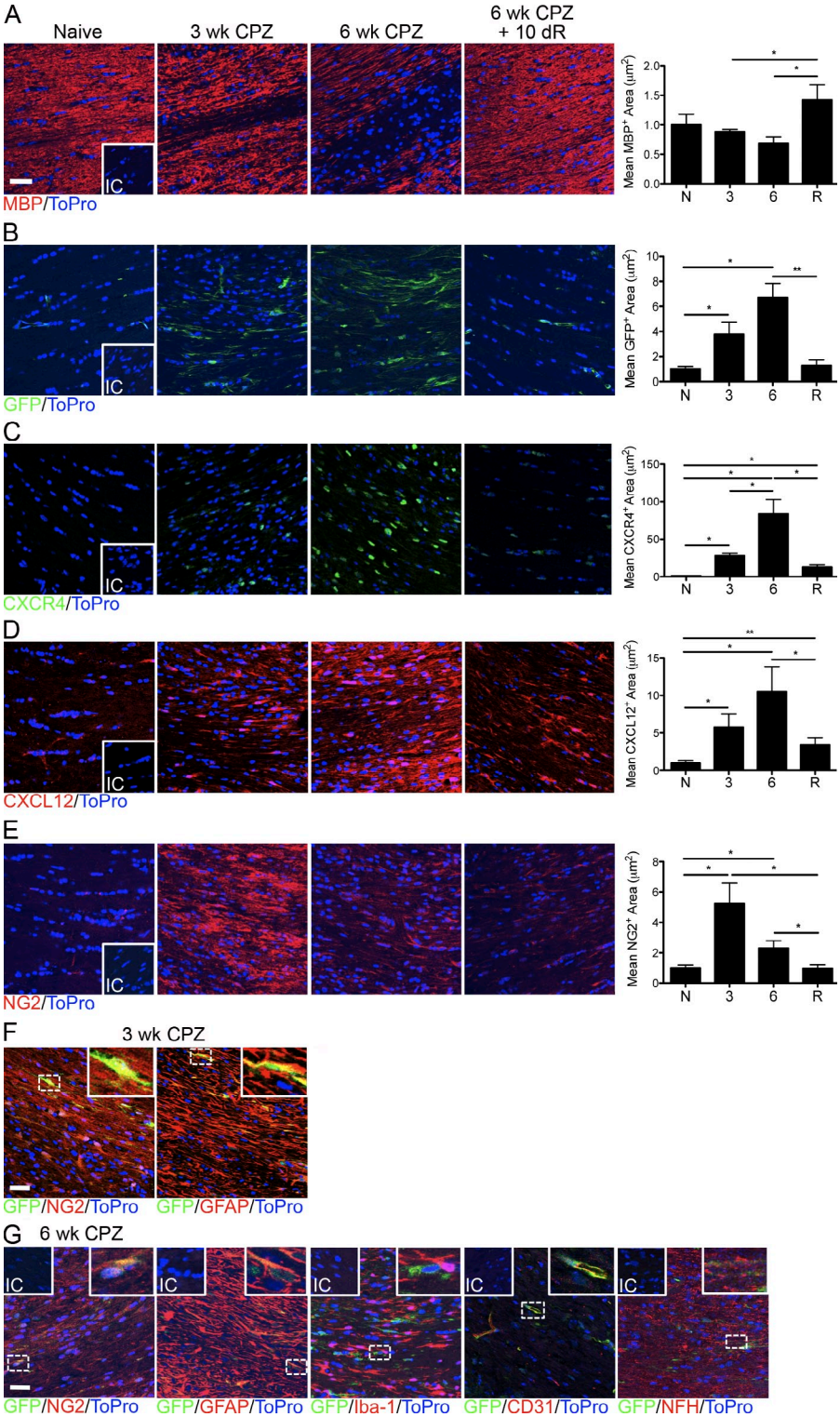

Figure 1. Chemokine expression and OPC population patterns throughout demyelination and remyelination. (A–E) Confocal IHC analysis of the CC of naive CXCR7$^{GFP/+}$ mice and after 3 or 6 wk of CPZ ingestion and after 10 d remyelination. Sections were stained for MBP (A), GFP (CXCR7; B), CXCR4 (C), CXCL12 (D), and NG2 (E). The mean positive area was analyzed for naive mice (N), mice fed CPZ for 3 or 6 wk, and mice fed CPZ for 6 wk and then a standard diet for a 10-d recovery period (R). (F and G) Confocal IHC analysis of the CC of CXCR7$^{GFP/+}$ mice after 3 wk (F) or 6 wk (G) of CPZ ingestion. Sections were stained for GFP (green) in combination with NG2, GFAP, Iba-1, CD31, and NFH (red). The area of co-localization was analyzed via Volocity image analysis software and normalized to the total GFP$^+$ area. Representative images are shown and quantitative data were collected from 3 sections per mouse (n = 4–8 mice/group) across 2 independent experiments with results shown as fold change compared with naive ± SEM. Insets = isotype control (IC). Bars, 25 μm. *, $P < 0.05$; **, $P < 0.01$.

(Fig. 3 A), as previously described (Patel et al., 2012). After the 3-wk treatment period, areas of hypercellularity in CXCR7 antagonist-treated animals were evident within the dorsal hippocampal commissure, which were absent in mice treated with vehicle (Fig. 3 B, white box). Analysis of BrdU$^+$NG2$^+$ OPC numbers revealed that CXCR7 antagonism led to a significant increase in the number of proliferating OPCs compared with vehicle-treated controls (Fig. 3 B, inset). Additionally, we observed similar MBP levels after simultaneous CPZ and vehicle or CCX771 treatment, suggesting demyelination was similar in the two treatment groups (Fig. 3 C). Numbers of proliferating OPCs in mice treated with vehicle

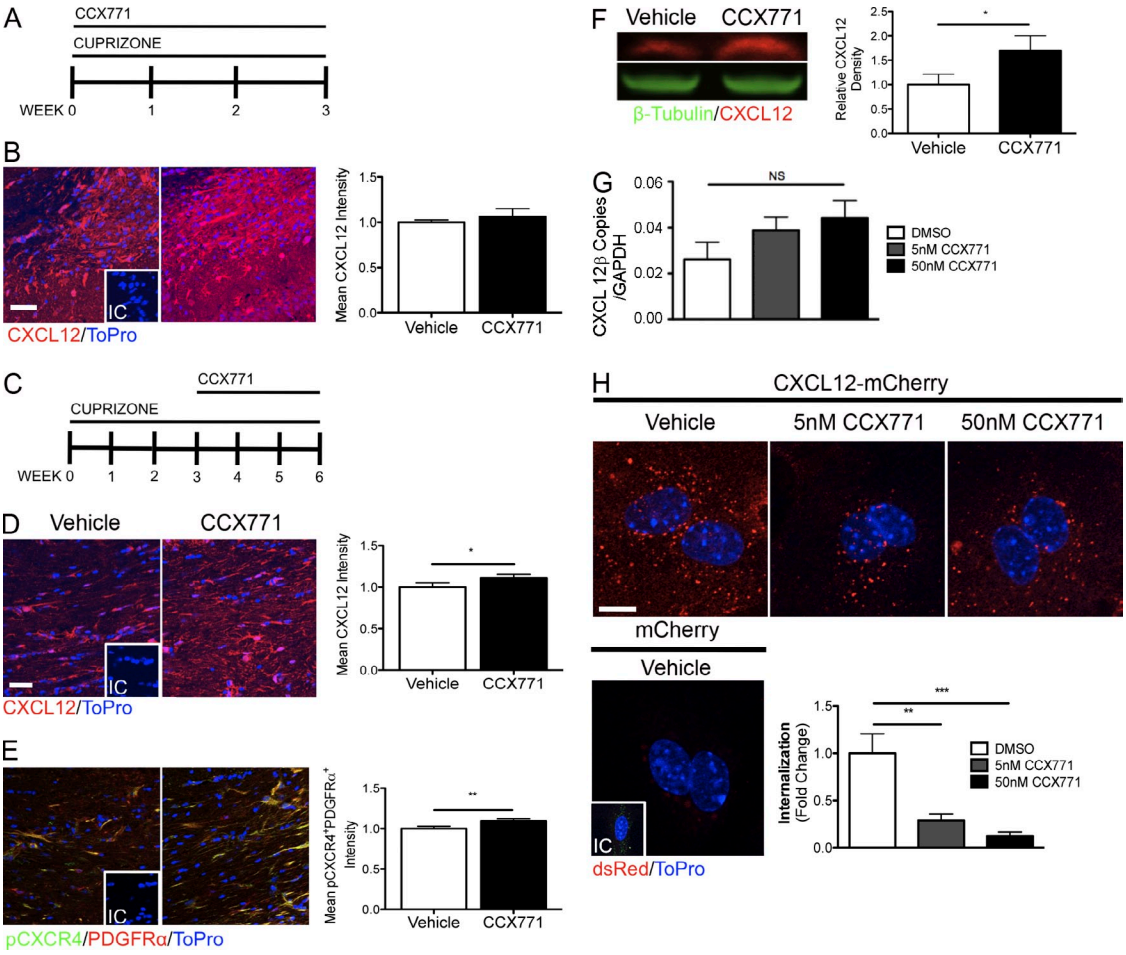

Figure 2. CXCR7 regulates CXCL12 expression during CNS demyelination. (A) Timeline depicting the experimental design for mice exposed to CPZ and vehicle or CCX771 treatment for 3 wk. (B) Confocal IHC analysis on sections of the CC stained for CXCL12 after 3 wk of CPZ ingestion and daily injections of vehicle or CCX771. The mean positive area was analyzed for vehicle- (white bar) and CCX771-treated (black bar) mice. Representative images are shown and quantitative data were collected from 3 sections per mouse (n = 4–5 mice/group) across 2 independent experiments. Insets = isotype control (IC). Bar, 25 µm. (C) Timeline depicting the experimental design for mice exposed to CPZ for 6 wk and vehicle or CCX771 treatment for 3 wk. (D and E) Confocal IHC analysis of the CC was done on sections that were stained for CXCL12 (D) and p-CXCR4 and PDGFRα (E). (F) CXCL12 protein levels within dissected caudal CC of treated mice were determined by Western blot. Quantitation of relative CXCL12 versus β-tubulin was performed (n = 4–5 mice/group). (G) Primary astrocytes were treated with the indicated doses of CCX771 and expression of CXCL12 was measured via qRT-PCR. Data are representative of 2 independent experiments, each group in 5 replicates. (H) Astrocytes were treated for 2 h with a vehicle control (DMSO) or with 5 or 50 nM CCX771 after a 4-h incubation with either CXCL12-mCherry or recombinant mCherry (25 ng/ml) in combination with vehicle or CCX771. The fold change in internalization was determined by confocal microscopy. Data are representative of 2 independent experiments, each group in 8 replicates with data shown as fold change over vehicle ± SEM. Inset = isotype control (IC). Bars, 10 µm. *, P ≤ 0.05; **, P ≤ 0.01; ***, P < 0.001.

or CCX771 for the final 3 wk of CPZ exposure (Fig. 3 D), as assessed via IHC for PDGFRα$^+$Ki-67$^+$ cells, were too few to quantitate (unpublished data).

Because CXCR7 mediates the internalization of CXCL12 (Fig. 2 H), thereby regulating CXCR4 activation in OPCs (Fig. 2 E), we hypothesized that therapeutic targeting of CXCR7 might impact OPC differentiation during demyelination. To test this, we administered CCX771 during the latter 3 wk of 6 wk of CPZ exposure (Fig. 3 D). Although there was a decrease in immature PDGFRα$^+$ cells (Fig. 3 F), we observed a significant increase in mature, GSTπ$^+$ oligodendrocytes (Fig. 3 H) in mice treated with CCX771 compared with those that received vehicle. Consistent with this, levels of myelin oligodendrocyte glycoprotein (MOG) and myelin staining were increased in CCX771-treated mice compared with those treated with vehicle (Fig. 3 I), although this did not reach statistical significance, presumably because of the continued presence of CPZ. Furthermore, using an antibody that detects MBP_{69-86}, a cryptic epitope which is normally unavailable for antibody binding in intact myelin (Matsuo et al., 1997), we found that mice treated with CCX771 revealed significantly less exposed MBP_{69-86} during CXCR7 antagonism (Fig. 3 J). These observations were confirmed using standard histological myelin staining

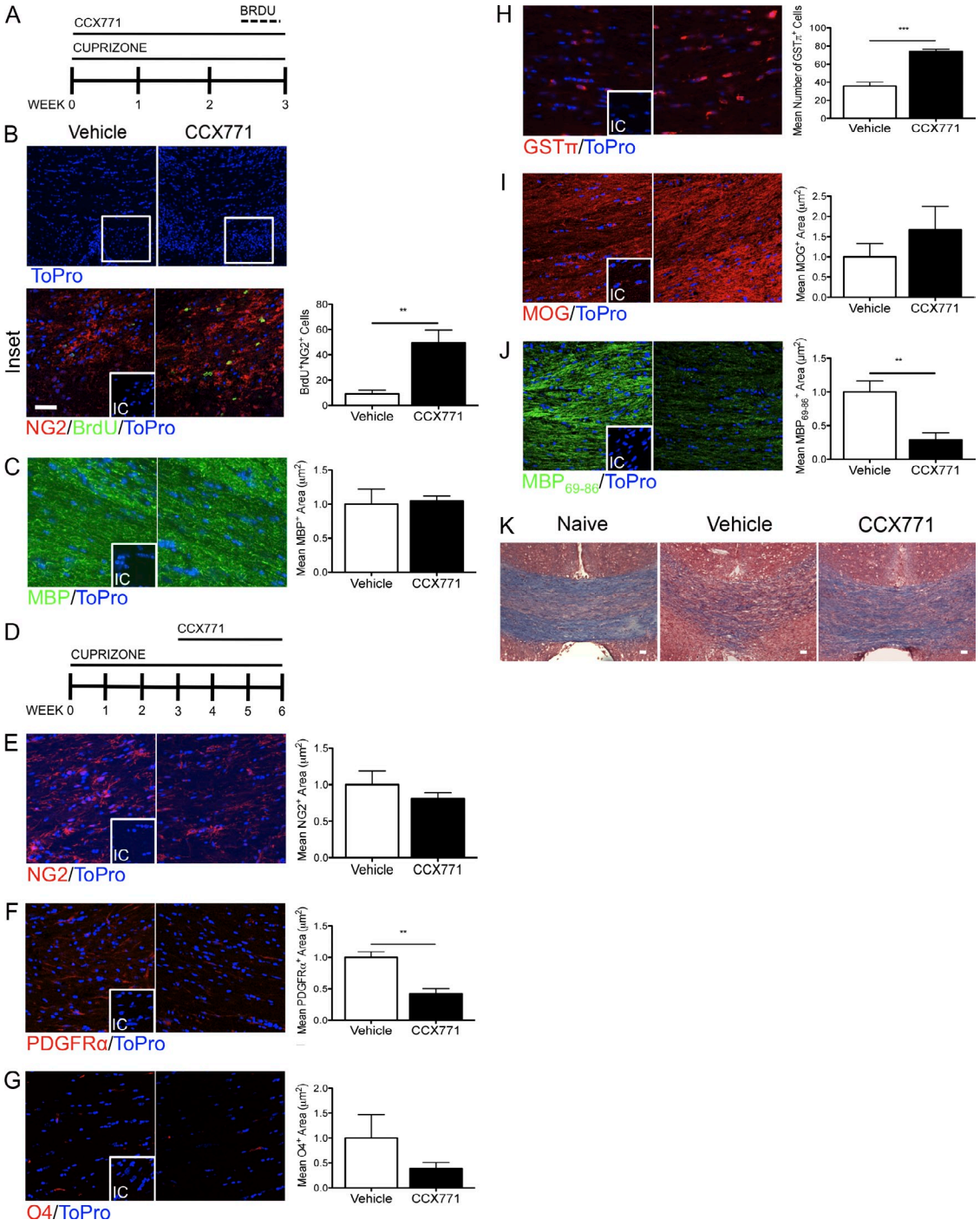

Figure 3. Inhibition of CXCR7 enhances OPC proliferation and maturation. (A) The depicted timeline represents the experimental design for mice given BrdU after vehicle or CCX771 treatment. (B and C) Confocal IHC analysis of the CC after 3 wk of CPZ ingestion and daily injections of vehicle or CCX771 s.c. (B) Sections of the CC delineated by the white box in B were stained for BrdU (green; B) and NG2 (red; B) or MBP (C). The mean number of $BrdU^+NG2^+$ cells/mouse was counted and mean positive areas of MBP immunostaining were analyzed across 3 sections for vehicle- (white bar) and CCX771-treated (black bar) mice. Representative images are shown and quantitative data were collected from 3 sections per mouse (n = 4–5 mice/group) across 2 independent experiments. Inset = isotype control (IC). Bars, 25 µm. (D) Timeline depicting the experimental design for mice exposed to CPZ for 6 wk and vehicle or CCX771 treatment for 3 wk. (E–J) Confocal IHC analysis of the CC was performed on sections that were stained for NG2 (E), PDGFRα (F), O4 (G), GSTπ (H), MOG (I), and MBP_{69-86} (J). The mean positive areas of immunostaining were analyzed for mice treated with vehicle (white bar) or CCX771 (black bar). Representative images are shown and quantitative data were collected from 3 sections per mouse (n = 8 mice/group) across 2 independent experiments with data shown as fold change over vehicle ± SEM. Inset = isotype control (IC); Bar, 25 µm. **, $P < 0.01$; ***, $P < 0.001$. (K) Eriochrome cyanine R staining of the CC for naive, vehicle- and CCX771-treated mice at 6 wk. Bars, 200 µm.

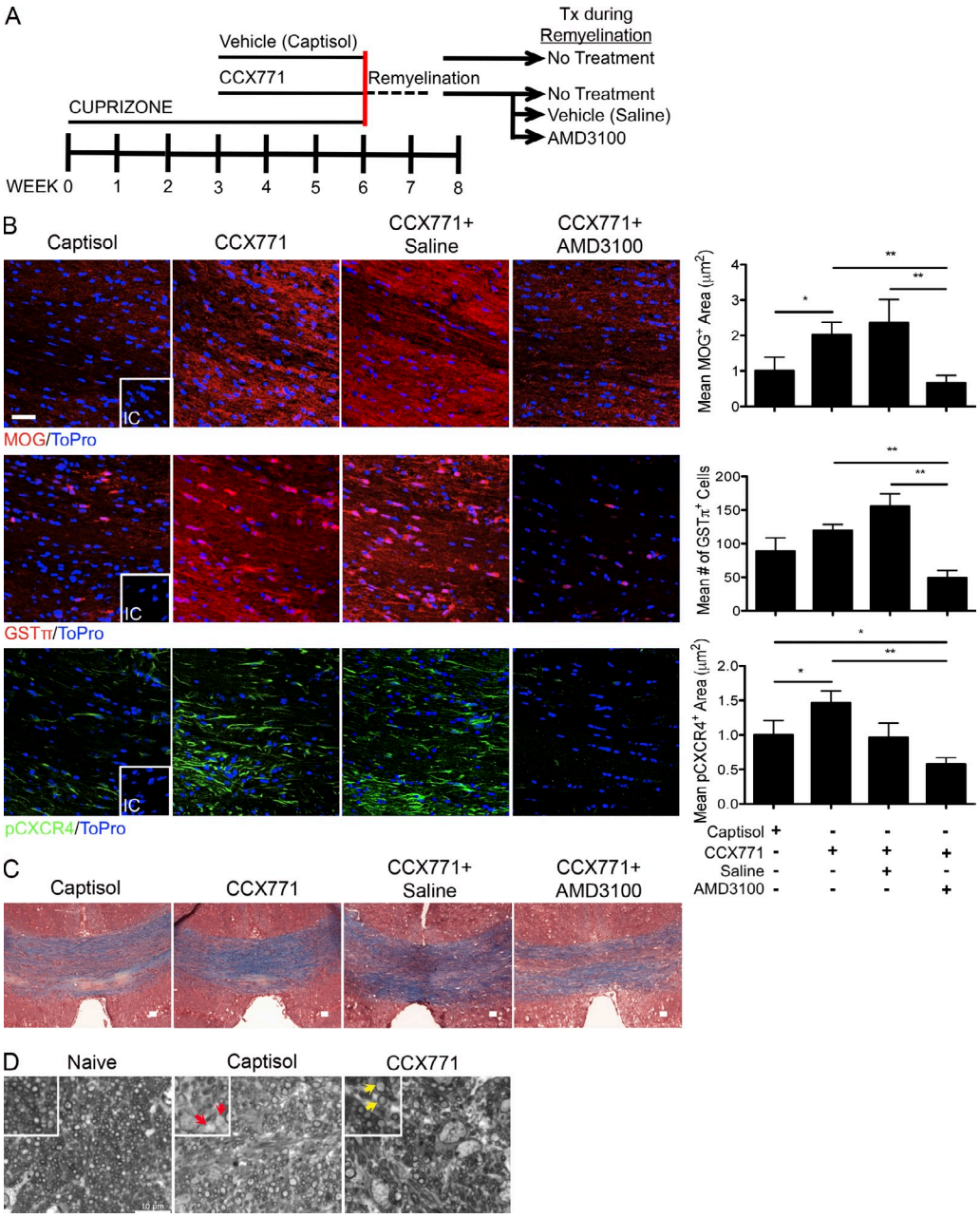

Figure 4. CXCR7 restricts CXCR4-mediated OPC maturation. (A) The depicted timeline represents the experimental design for mice given CPZ for 6 wk and captisol or CCX771 for 3 wk. After the CPZ/captisol or CCX771 treatments, mice were fed a standard chow and captisol and CCX771 injections were ceased as depicted by the red line. During this recovery period, mice received continuous infusion of saline or AMD3100 versus no treatment for 10 d. (B) Quantitative confocal imaging of immunostained CC sections for MOG, GSTπ, and pCXCR4. Data are expressed as the mean positive area (MOG and pCXCR4) or mean number of cells (GSTπ) for mice treated with captisol, CCX771 alone, CCX771 and saline, and CCX771 and AMD3100. Representative images are shown and quantitative data were collected from 3 sections per mouse (n = 5–10 mice/group) across 2 independent experiments with data shown as fold change over captisol ± SEM. Inset = isotype control (IC). Bar, 25 µm. *, $P < 0.05$; **, $P < 0.01$. (C) Eriochrome cyanine R staining on sections of the CC from captisol-, CCX771-, CCX771 and saline–, and CCX771 and AMD3100–treated mice. Bars, 200 µm. (D) Toluidine blue staining on sagittal sections of the CC from naive (left), captisol-treated (middle), and CCX771-treated (right) mice with digitally zoomed images (inset). Red arrows = demyelinated axons, yellow arrows = remyelinated axons. Bar, 10 µm. Representative images are shown (n = 4 mice/group).

(Fig. 3 K). These data suggest that CXCR7 regulates CXCR4 signaling on OPCs, controlling the kinetics of their differentiation and myelin recovery within injured white matter of the adult CNS.

Remyelination is regulated by CXCR7

To assess OPC maturation during remyelination, we fed mice a CPZ-infused diet for 6 wk, antagonizing CXCR7 during weeks 3–6. We then discontinued both the CPZ and CCX771

treatments and allowed mice to remyelinate for 10 d (Fig. 4 A). After the remyelination phase, mice treated with the CXCR7 antagonist had increased MOG expression and GSTπ^+ cells within the CC compared with those treated with vehicle (Fig. 4 B). To determine if the increased myelin expression observed during CXCR7 blockade was due to increased CXCR4 activation (Fig. 3), mice were continuously administered the specific CXCR4 antagonist AMD3100 versus saline vehicle for 10 d after the cessation of CPZ and CCX771 (Fig. 4 A). As expected, during remyelination of the CC, mice treated with CCX771, followed by vehicle, exhibited similar oligodendrocyte maturation patterns as those treated with CCX771 alone. However, when mice were additionally treated with AMD3100 during remyelination, levels of MOG expression and numbers of GSTπ^+ cells were similar to mice treated with vehicle (Fig. 4 B). Furthermore, we determined that increased remyelination correlated with phosphorylation of CXCR4 (Fig. 4 B). Remyelination was confirmed using eriochrome cyanine staining of coronal sections of the CC (Fig. 4 C). Toluidine blue staining of sagittal sections of the CC additionally revealed the increased presence of new myelin in CCX771-treated mice (Fig. 4 D, yellow arrows) in comparison with those of vehicle-treated mice, which contained more demyelinated axons (Fig. 4 D, red arrows). Collectively, these data suggest that CXCR4-dependent remyelination in the adult CNS is enhanced after CXCR7 antagonism.

Repair of demyelinated lesions is necessary to prevent irreversible neurological disability in MS patients and requires the proliferation and maturation of OPCs within the CNS. Several potential targets for promoting myelination have been described; however, here, for the first time, we were able to therapeutically enhance remyelination after CNS injury using a small molecule inhibitor to prompt activation of development-like chemokine networks.

The up-regulation of CXCR7 exclusively during demyelination is consistent with its role in tightly regulating CXCR4 activity in response to extracellular CXCL12 during CNS insult. In other CNS injury models, including cerebral ischemia, CXCR7 mRNA was elevated in neurons after middle cerebral artery occlusion and was undetectable once tissue degeneration was complete and cell-based regeneration was initiated (Schönemeier et al., 2008). Widespread expression of CXCR7 suggests that the regulation of CXCL12 availability is critical for the function of CXCR4. During neuroinflammation, CXCR4 is expressed on neural progenitor cells and facilitates migration to sites of pathology, namely via directed expression of CXCL12 on the surface of astrocytes and CNS endothelial cells (Imitola et al., 2004). The interplay of the two CXCL12 receptors during OPC maturation becomes evident as CXCR7 protein expression increases while CXCR4 expression decreases during differentiation (Göttle et al., 2010), indicating that CXCR7 has an opposing, and likely regulatory, role in CXCR4-mediated OPC maturation.

In a viral model of demyelination, CXCR4 signaling was indispensable for OPC proliferation and enhanced remyelination (Carbajal et al., 2011). Furthermore, AMD3100 treatment during CPZ-induced demyelination specifically reduces the number of proliferating, white matter-associated NG2$^+$ OPCs (Patel et al., 2012). Here, our results demonstrate that CXCR7 works to restrict CXCL12 availability, limiting the pool of OPCs in areas of demyelination. Hence, blocking CXCR7 activity resulted in expansion of remyelination-competent cells that may participate in recovery.

Targeting of CXCR7 to regulate extracellular CXCL12 and CXCR4 activation has significant implication for the treatment of chronic CNS demyelinating diseases such as MS. During MS pathogenesis, OPCs are more abundant on lesion borders versus normal-appearing white matter and are phenotypically quiescent, lacking markers of proliferation and maturation (Wolswijk, 1998; Kuhlmann et al., 2008). Furthermore, astrocyte-associated CXCL12 is expressed on chronic lesion borders at low to moderate levels compared with in active lesions (Calderon et al., 2006; Kuhlmann et al., 2008), suggesting that in chronic lesions, OPCs are locally associated with astrocyte CXCL12 to enhance CXCR4 activation. Although the mechanisms underlying CXCR4-mediated OPC maturation are poorly understood, growth factors, including brain-derived neurotropic factor (BDNF), may contribute to CXCR4 expression or activation, as exposure to BDNF renders OPCs responsive to CXCL12 (Xu and Heilshorn, 2013).

Current treatment modalities for MS primarily rely on immune suppression, which can lead to unfavorable side effects. Furthermore, we and others have shown that inflammatory mediators, like tumor necrosis factor α, promote CNS repair (Arnett et al., 2001; Patel et al., 2012). Importantly, we have demonstrated that the use of a CXCR7 antagonist during demyelination has proven beneficial not only in the context of repair, as shown here, but also during immune-mediated CNS injury, while leaving immune cell function largely intact (Cruz-Orengo et al., 2011b). Together, these data emphasize the potential efficacy of CXCR7 antagonism during initial inflammatory events as well as during recovery in MS patients.

MATERIALS AND METHODS

Mouse model of CPZ-mediated demyelination. 8-wk-old male C57BL/6 or CXCR7$^{GFP/+}$ mice were fed a standard diet (Harlan) containing 0.2% CPZ (Sigma-Aldrich) for 3–6 wk. For the induction of remyelination, CPZ-infused feed was removed and animals were given standard chow for 10 d. All animal studies were performed in accordance with the Animal Care and Use Committee guidelines of the National Institutes of Health and were conducted under protocols approved by the Animal Care and Use Committee of Washington University.

Antibodies. The following antibodies were used in this study: anti-MBP (1:100; Abcam), -MBP$_{69\text{-}86}$ (1:2000; Millipore), -GFP (1:1,000; Invitrogen), -CXCR4 (1:50; Abcam), -CXCL12β (1:20; eBioscience), -NG2 (1:100; Millipore), -GFAP (1:200; Invitrogen), –Iba-1 (1:250; Wako), -CD31 (1:20; BD), –neurofilament heavy chain (NFH; 1:500; Aves), –phospho-339S-CXCR4 (1:50; Abcam), -PDGFRα (1:50; Millipore), -GSTπ (1:1,000; Assay Designs), -BrdU (1:100; Sigma-Aldrich), and -MOG (1:100; R&D Systems).

Immunohistochemistry. Frozen sections were prepared and detection of cell markers were accomplished as previously described (Patel et al., 2010, 2012). In brief, tissue sections were blocked with goat serum and Triton X-100 (Sigma-Aldrich) for 1 h at room temperature and then exposed to primary

antibody overnight at 4°C. For MBP and pCXCR4 labeling, we used an antigen retrieval solution consisting of 0.1% trypsin and 0.1% CaCl in 0.05 M Tris, pH 7.4, and 10 mM citrate buffer, pH 6.0, respectively, at 37°C for 10 min, and for BrdU labeling, 1 M HCl was applied to tissue sections for 25 min at 45°C. Secondary antibodies conjugated to Alexa Fluor 488 or Alexa Fluor 555 (Molecular Probes) were applied for 1 h at room temperature. Nuclei were counterstained with ToPro3 (Molecular Probes) diluted in PBS. Sections were analyzed using the 40× objective of a confocal laser-scanning microscope (LSM 510 META; Carl Zeiss). The mean positive area and intensity thresholds were determined using appropriate isotype control antibodies and were quantified using AxioVision (Carl Zeiss) and Volocity (Perkin Elmer) image analysis software.

In vivo BrdU incorporation. 50 mg/kg BrdU (Sigma-Aldrich) in PBS was injected i.p. every 8 h for 4 d as previously described (Arnett et al., 2001; Patel et al., 2012).

In vivo CCX771 and AMD3100 treatment. 30 mg/kg CCX771 (ChemoCentryx) or vehicle (10% Captisol) was administered daily (s.c.) in 100 µl vehicle throughout the treatment period. Continuous dose treatment of AMD3100 (50 µg/h; Sigma-Aldrich) or saline was achieved using 14-d osmotic pumps (Alzet) with an infusion rate of 0.25 µl/h as previously described (Patel et al., 2010).

Histology. For eriochrome cyanine staining, frozen sections of the CC were rehydrated in PBS, followed by dH_2O and stained with Eriochrome cyanine R (Sigma-Aldrich) for 10 min. Tissue was then rinsed in tap water for 5 min and differentiated in 10% iron alum (Sigma-Aldrich). Sections were then counterstained with van Gieson stain, washed, and dehydrated before visualization. For toluidine blue staining, brains were immersion fixed in 2% PFA and 2.5% glutaraldehyde in 0.1 M sodium cacodylate, pH 7.4. A 1.0-mm cube of the caudal CC was dissected and washed in 0.1 M sodium cacodylate overnight. Tissue was then fixed for 2 h in 1% osmium tetroxide and washed overnight in 0.1 M sodium cacodylate. The tissue was dehydrated in ethanol, infiltrated with 1:1 Spurr's resin/100% ethanol, embedded in Spurr's resin, allowed to polymerize for 48 h at 65°C, and sagittal 1-µm-thick sections were cut with a diamond knife. Sections were stained with toluidine blue for 1–2 min over heat, rinsed with tap water, and coverslips were applied.

Western blot. The caudal CC was dissected and 10 µg protein lysates were isolated using RIPA buffer supplemented with a protease and phosphatase-3 inhibitor cocktail (Sigma-Aldrich). Lysates were resolved on a 4–12% Bis-Tris gel and transferred onto an iBlot Nitrocellulose transfer membrane (Invitrogen) according to standard protocols. Blots were probed with polyclonal rabbit anti-CXCL12β (eBioscience) and monoclonal mouse anti–β-tubulin (Sigma-Aldrich) antibodies, followed by incubation with IRDye-conjugated secondary antibodies (LI-COR). Blots were imaged using the Odyssey fluorescent scanning system (LI-COR) and analyzed using ImageJ (National Institutes of Health).

Quantitative PCR. Astrocytes were isolated from postnatal day 3 C57BL/6 mouse pups as previously described (Patel et al., 2010). Cells were seeded in 24-well plates until confluent and treated with DMSO or CCX771 for 24 h. Total RNA was isolated and quantitative real-time (qRT) PCR was performed using primers for CXCL12β as previously described (McCandless et al., 2006).

In vitro CXCL12-mCherry internalization. Astrocytes were seeded in 24-well plates until confluent and treated with DMSO or CCX771 for 2 h. CXCL12-mCherry fusion protein (Cruz-Orengo et al., 2011b) or recombinant mCherry (BioVision) was then added to the cultures for 4 h. Cells were then washed with cold 0.5 M acetic acid wash buffer to remove surface bound CXCL12-mCherry, and then fixed with ice-cold 4% PFA. Astrocytes were then labeled with polyclonal rabbit anti-DsRed (1:200; Takara Bio Inc.) and counterstained with ToPro3 as previously described (Cruz-Orengo et al., 2011b).

Statistical analysis. Data were analyzed using Prism (GraphPad Software). An unpaired Student's *t* test or one-way ANOVA was used to determine statistical significance. Data are expressed as means ± SEM. Sample sizes are indicated in the figure legends.

The authors thank Megan Muccigrosso and Bryan Bollman for technical assistance and Mark Penfold (ChemoCentryx) for CCX771.

This study was supported by the W.M. Keck Fellowship in Molecular Medicine (J.L. Williams), the National Institutes of Health/National Institute of Neurological Disorders and Stroke Grant P01 NS059560 (R.S. Klein), and grants from the National Multiple Sclerosis Society (R.S. Klein).

The authors declare no competing financial interests.

Submitted: 11 June 2013
Accepted: 19 March 2014

REFERENCES

Arnett, H.A., J. Mason, M. Marino, K. Suzuki, G.K. Matsushima, and J.P. Ting. 2001. TNFα promotes proliferation of oligodendrocyte progenitors and remyelination. *Nat. Neurosci.* 4:1116–1122. http://dx.doi.org/10.1038/nn738

Bajetto, A., R. Bonavia, S. Barbero, P. Piccioli, A. Costa, T. Florio, and G. Schettini. 1999. Glial and neuronal cells express functional chemokine receptor CXCR4 and its natural ligand stromal cell-derived factor 1. *J. Neurochem.* 73:2348–2357. http://dx.doi.org/10.1046/j.1471-4159.1999.0732348.x

Banisadr, G., D. Skrzydelski, P. Kitabgi, W. Rostène, and S.M. Parsadaniantz. 2003. Highly regionalized distribution of stromal cell-derived factor-1/CXCL12 in adult rat brain: constitutive expression in cholinergic, dopaminergic and vasopressinergic neurons. *Eur. J. Neurosci.* 18:1593–1606. http://dx.doi.org/10.1046/j.1460-9568.2003.02893.x

Boldajipour, B., H. Mahabaleshwar, E. Kardash, M. Reichman-Fried, H. Blaser, S. Minina, D. Wilson, Q. Xu, and E. Raz. 2008. Control of chemokine-guided cell migration by ligand sequestration. *Cell.* 132:463–473. http://dx.doi.org/10.1016/j.cell.2007.12.034

Calderon, T.M., E.A. Eugenin, L. Lopez, S.S. Kumar, J. Hesselgesser, C.S. Raine, and J.W. Berman. 2006. A role for CXCL12 (SDF-1α) in the pathogenesis of multiple sclerosis: regulation of CXCL12 expression in astrocytes by soluble myelin basic protein. *J. Neuroimmunol.* 177:27–39. http://dx.doi.org/10.1016/j.jneuroim.2006.05.003

Carbajal, K.S., C. Schaumburg, R. Strieter, J. Kane, and T.E. Lane. 2010. Migration of engrafted neural stem cells is mediated by CXCL12 signaling through CXCR4 in a viral model of multiple sclerosis. *Proc. Natl. Acad. Sci. USA.* 107:11068–11073. http://dx.doi.org/10.1073/pnas.1006375107

Carbajal, K.S., J.L. Miranda, M.R. Tsukamoto, and T.E. Lane. 2011. CXCR4 signaling regulates remyelination by endogenous oligodendrocyte progenitor cells in a viral model of demyelination. *Glia.* 59:1813–1821. http://dx.doi.org/10.1002/glia.21225

Chang, A., A. Nishiyama, J. Peterson, J. Prineas, and B.D. Trapp. 2000. NG2-positive oligodendrocyte progenitor cells in adult human brain and multiple sclerosis lesions. *J. Neurosci.* 20:6404–6412.

Chang, A., W.W. Tourtellotte, R. Rudick, and B.D. Trapp. 2002. Premyelinating oligodendrocytes in chronic lesions of multiple sclerosis. *N. Engl. J. Med.* 346:165–173. http://dx.doi.org/10.1056/NEJMoa010994

Compston, A., and A. Coles. 2002. Multiple sclerosis. *Lancet.* 359:1221–1231. http://dx.doi.org/10.1016/S0140-6736(02)08220-X

Cruz-Orengo, L., Y.J. Chen, J.H. Kim, D. Dorsey, S.K. Song, and R.S. Klein. 2011a. CXCR7 antagonism prevents axonal injury during experimental autoimmune encephalomyelitis as revealed by in vivo axial diffusivity. *J. Neuroinflammation.* 8:170. http://dx.doi.org/10.1186/1742-2094-8-170

Cruz-Orengo, L., D.W. Holman, D. Dorsey, L. Zhou, P. Zhang, M. Wright, E.E. McCandless, J.R. Patel, G.D. Luker, D.R. Littman, et al. 2011b. CXCR7 influences leukocyte entry into the CNS parenchyma by controlling abluminal CXCL12 abundance during autoimmunity. *J. Exp. Med.* 208:327–339. http://dx.doi.org/10.1084/jem.20102010

Dziembowska, M., T.N. Tham, P. Lau, S. Vitry, F. Lazarini, and M. Dubois-Dalcq. 2005. A role for CXCR4 signaling in survival and migration of neural and oligodendrocyte precursors. *Glia.* 50:258–269. http://dx.doi.org/10.1002/glia.20170

Franklin, R.J., and C. Ffrench-Constant. 2008. Remyelination in the CNS: from biology to therapy. *Nat. Rev. Neurosci.* 9:839–855. http://dx.doi.org/10.1038/nrn2480

Göttle, P., D. Kremer, S. Jander, V. Odemis, J. Engele, H.P. Hartung, and P. Küry. 2010. Activation of CXCR7 receptor promotes oligodendroglial cell maturation. *Ann. Neurol.* 68:915–924. http://dx.doi.org/10.1002/ana.22214

Hatse, S., K. Princen, G. Bridger, E. De Clercq, and D. Schols. 2002. Chemokine receptor inhibition by AMD3100 is strictly confined to CXCR4. *FEBS Lett.* 527:255–262. http://dx.doi.org/10.1016/S0014-5793(02)03143-5

Imitola, J., K. Raddassi, K.I. Park, F.J. Mueller, M. Nieto, Y.D. Teng, D. Frenkel, J. Li, R.L. Sidman, C.A. Walsh, et al. 2004. Directed migration of neural stem cells to sites of CNS injury by the stromal cell-derived factor 1α/CXC chemokine receptor 4 pathway. *Proc. Natl. Acad. Sci. USA.* 101:18117–18122. http://dx.doi.org/10.1073/pnas.0408258102

Klein, R.S., and J.B. Rubin. 2004. Immune and nervous system CXCL12 and CXCR4: parallel roles in patterning and plasticity. *Trends Immunol.* 25:306–314. http://dx.doi.org/10.1016/j.it.2004.04.002

Kuhlmann, T., V. Miron, Q. Cui, C. Wegner, J. Antel, and W. Brück. 2008. Differentiation block of oligodendroglial progenitor cells as a cause for remyelination failure in chronic multiple sclerosis. *Brain.* 131:1749–1758. http://dx.doi.org/10.1093/brain/awn096

Lindner, M., S. Heine, K. Haastert, N. Garde, J. Fokuhl, F. Linsmeier, C. Grothe, W. Baumgärtner, and M. Stangel. 2008. Sequential myelin protein expression during remyelination reveals fast and efficient repair after central nervous system demyelination. *Neuropathol. Appl. Neurobiol.* 34:105–114.

Matsuo, A., G.C. Lee, K. Terai, K. Takami, W.F. Hickey, E.G. McGeer, and P.L. McGeer. 1997. Unmasking of an unusual myelin basic protein epitope during the process of myelin degeneration in humans: a potential mechanism for the generation of autoantigens. *Am. J. Pathol.* 150:1253–1266.

McCandless, E.E., Q. Wang, B.M. Woerner, J.M. Harper, and R.S. Klein. 2006. CXCL12 limits inflammation by localizing mononuclear infiltrates to the perivascular space during experimental autoimmune encephalomyelitis. *J. Immunol.* 177:8053–8064.

McCandless, E.E., L. Piccio, B.M. Woerner, R.E. Schmidt, J.B. Rubin, A.H. Cross, and R.S. Klein. 2008. Pathological expression of CXCL12 at the blood-brain barrier correlates with severity of multiple sclerosis. *Am. J. Pathol.* 172:799–808. http://dx.doi.org/10.2353/ajpath.2008.070918

Naumann, U., E. Cameroni, M. Pruenster, H. Mahabaleshwar, E. Raz, H.G. Zerwes, A. Rot, and M. Thelen. 2010. CXCR7 functions as a scavenger for CXCL12 and CXCL11. *PLoS ONE.* 5:e9175. http://dx.doi.org/10.1371/journal.pone.0009175

Patel, J.R., E.E. McCandless, D. Dorsey, and R.S. Klein. 2010. CXCR4 promotes differentiation of oligodendrocyte progenitors and remyelination. *Proc. Natl. Acad. Sci. USA.* 107:11062–11067. http://dx.doi.org/10.1073/pnas.1006301107

Patel, J.R., J.L. Williams, M.M. Muccigrosso, L. Liu, T. Sun, J.B. Rubin, and R.S. Klein. 2012. Astrocyte TNFR2 is required for CXCL12-mediated regulation of oligodendrocyte progenitor proliferation and differentiation within the adult CNS. *Acta Neuropathol.* 124:847–860. http://dx.doi.org/10.1007/s00401-012-1034-0

Schönemeier, B., S. Schulz, V. Hoellt, and R. Stumm. 2008. Enhanced expression of the CXCl12/SDF-1 chemokine receptor CXCR7 after cerebral ischemia in the rat brain. *J. Neuroimmunol.* 198:39–45. http://dx.doi.org/10.1016/j.jneuroim.2008.04.010

Steinman, L. 2009. A molecular trio in relapse and remission in multiple sclerosis. *Nat. Rev. Immunol.* 9:440–447. http://dx.doi.org/10.1038/nri2548

Wolswijk, G. 1998. Chronic stage multiple sclerosis lesions contain a relatively quiescent population of oligodendrocyte precursor cells. *J. Neurosci.* 18:601–609.

Xu, H., and S.C. Heilshorn. 2013. Microfluidic investigation of BDNF-enhanced neural stem cell chemotaxis in CXCL12 gradients. *Small.* 9:585–595. http://dx.doi.org/10.1002/smll.201202208

Zhu, Y., T. Matsumoto, S. Mikami, T. Nagasawa, and F. Murakami. 2009. SDF1/CXCR4 signalling regulates two distinct processes of precerebellar neuronal migration and its depletion leads to abnormal pontine nuclei formation. *Development.* 136:1919–1928. http://dx.doi.org/10.1242/dev.032276

Zou, Y.R., A.H. Kottmann, M. Kuroda, I. Taniuchi, and D.R. Littman. 1998. Function of the chemokine receptor CXCR4 in haematopoiesis and in cerebellar development. *Nature.* 393:595–599. http://dx.doi.org/10.1038/31269